Proc. Natl. Acad. Sci. USA
Vol. 93, pp. 11985–11990, October 1996
Neurobiology

Modeling back propagating action potential in weakly excitable dendrites of neocortical pyramidal cells

(compartmental model/action potential initiation site)

M. RAPP, Y. YAROM, AND I. SEGEV*

Department of Neurobiology, Institute of Life Sciences and Center for Neural Computation, The Hebrew University, Jerusalem 91904, Israel

Communicated by B. Sakmann, Max-Planck-Institut für Medizinische Forschung, Heidelberg, Germany, July 30, 1996 (received for review April 5, 1995)

ABSTRACT **Simultaneous recordings from the soma and apical dendrite of layer V neocortical pyramidal cells of young rats show that, for any location of current input, an evoked action potential (AP) always starts at the axon and then propagates actively, but decrementally, backward into the dendrites. This back-propagating AP is supported by a low density ($\bar{g}_{Na} = \approx 4$ mS/cm^2) of rapidly inactivating voltage-dependent Na^+ channels in the soma and the apical dendrite. Investigation of detailed, biophysically constrained, models of reconstructed pyramidal cells shows the following. (*i*) The initiation of the AP first in the axon cannot be explained solely by morphological considerations; the axon must be more excitable than the soma and dendrites. (*ii*) The minimal Na^+ channel density in the axon that fully accounts for the experimental results is about 20-times that of the soma. If $\bar{g}_{Na}$ in the axon hillock and initial segment is the same as in the soma {as recently suggested by Colbert and Johnston [Colbert, C. M. & Johnston, D. (1995) Soc. Neurosci. Abstr. 21, 684.2]}, then $\bar{g}_{Na}$ in the more distal axonal regions is required to be about 40-times that of the soma. (*iii*) A backward propagating AP in weakly excitable dendrites can be modulated in a graded manner by background synaptic activity. The functional role of weakly excitable dendrites and a more excitable axon for forward synaptic integration and for backward, global, communication between the axon and the dendrites is discussed.**

Dendrites are fine, highly branched processes that serve as the major receptive area for synaptic connections. Most of the input–output functions of the neuron are carried out in the dendrites and these functions depend critically on the electrical properties of the dendritic membrane (1, 2). Application of advanced electrophysiological, optical, and molecular methods have revealed that the dendritic membrane of many neuron types have a variety of voltage-dependent ion channels and, consequently, dendrites are nonlinear electrical devices (3–8). Theoretical studies have demonstrated that voltage-dependent dendritic channels could significantly enrich the computational capabilities of the neuron and that these computations critically depend on the type, kinetics, and density of the excitable channels (9–12).

The novel infrared video-microscopy technique applied to brain slices (13) permits excision of membrane patches from well-identified dendritic locations so that direct measurements of the electrical properties of the channels embedded in these patches can be made (14–16). Using this method, Stuart and Sakmann (14) found rapidly inactivating voltage-dependent Na^+ channels in the apical trunk of layer V neocortical pyramidal cells of the young rat (see also Fig. 1). These channels seem to be *uniformly* distributed at low density (equivalent to ≈ 4 mS/cm^2, or 1/30 the density found in the squid giant axon) over the apical dendrite and the soma. Simultaneous whole-cell recordings from the soma (or axon), and the apical dendrite have shown that, independent of synaptic input location, the sodium action potential (AP) is always initiated in the axon and then propagates actively, yet decrementally, backwards into the dendrite. Similar results were also reported recently in hippocampal CA1 pyramidal cells (17) and substantia nigra neurons (18).

These results raise several fundamental questions that we have explored in a simulation study. The first stage in this study was to construct a minimal model that mimics the behavior of the AP at the axon, soma and dendrites of a cortical neuron, and that is compatible with its morphology and (passive and active) biophysical characteristics. This model explains why the AP is always initiated first at the axon, showing whether this is the consequence of the morphological design of neocortical pyramidal cells, or the result of some electrical nonuniformity. A related question is why the AP propagates backward (from soma to the dendrite) rather than forward (from the dendrites to soma)? At the next stage the model was utilized to explore the following. (*i*) What could be the range of Na^+ channel density and kinetics in the axon? (*ii*) To what extent the back-propagating AP invades the basal tree? and (*iii*) How resistant the back-propagating AP is to background synaptic activity? Being decremental, one would intuitively assume that such an action potential could be easily blocked by the shunting effect of the massive background synaptic activity that exists in the *in vivo* condition (19–21). The predictions of the model are discussed together with the implications of the results for information processing in neocortical pyramidal neurons.

MODEL

Numerical computations were performed using the simulator NEURON (22). Large layer V pyramidal cells from the somatosensory cortex of 14-day-old rats were modeled. Four anatomically and physiologically characterized cells were used; the results presented here are related to the neuron depicted in Fig. 1, with similar results for the other three modeled cells (not shown). In the modeled cell in Fig. 1, the apical dendrite extends to about 1 mm from the soma. The basal tree consists of five short (150–220 μm) dendrites (20 dendritic terminals). The part of the axon that lies within the slice was also reconstructed; its total length is 1985 μm. Near the soma the axon diameter is 2.8 μm; it then reduces to about 0.5 μm in the fine collaterals of the axon. The total area of the dendrites and soma (excluding dendritic spines) was 37,047 μm^2 (7821 μm^2 in the basal tree, 25,780 μm^2 in the apical tree and 3446 μm^2 in the soma). The area of the reconstructed axon was 4917

The publication costs of this article were defrayed in part by page charge payment. This article must therefore be hereby marked "*advertisement*" in accordance with 18 U.S.C. §1734 solely to indicate this fact.

Abbreviations: EPSP, excitatory postsynaptic potential; AMPA, L-α-amino-3-hydroxy-5-methyl-4-isoxazolepropionate; NMDA, *N*-methyl-D-aspartate; GABA, γ-aminobutyric acid; AP, action potential.

*To whom reprint requests should be addressed. e-mail: idan@lobster.ls.huji.ac.il.

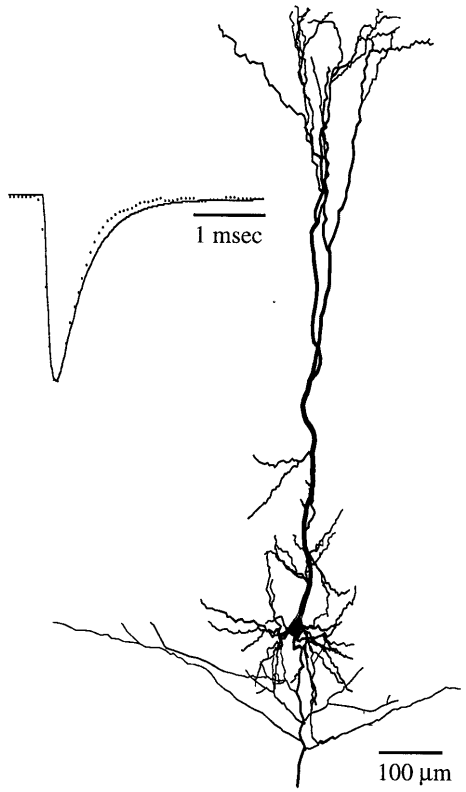

FIG. 1. Modeled layer V pyramidal cell. The neuron from the somatosensory cortex of 14-day-old rat was filled with biocytin and reconstructed using Neuron Tracing System (Eutectic). (*Inset*) Dotted line shows the rapidly inactivating Na^+ current measured by Stuart and Sakmann (14) in an excised dendritic patch; the continuous line shows the simulated Na^+ current. In both experiments and model, the current was evoked by a voltage step from −90 mV to −10 mV. With $\bar{g}_{Na} = 4$ mS/cm^2, this voltage step yields a peak Na^+ current of 3 pA/μm^2.

μm^2. Dendritic spines were distributed at the different dendritic segments in accordance to the measurements by Larkman (23). This yields a total of 11,982 spines for the modeled cell in Fig. 1. Assuming an area of 1.5 μm^2 for each spine, the total spine area was 17,937 μm^2 (33% of the total soma and dendritic area). Dendritic spines that were not directly activated by synaptic inputs were incorporated globally into the dendrites (21, 24). The dendritic spine membrane was assumed to be passive (25). A total of 1202 compartments were used to represent the dendritic tree, and the axon was modeled with 259 compartments. The soma was modeled as an isopotential compartment.

In addition to the morphology, strict physiological constraints should also be met by this model. First, the *passive* properties of cortical pyramidal cells were carefully measured. Specifically, by "peeling" the tail of soma transients, either those of somatic excitatory postsynaptic potentials (EPSPs) or resulting from current injection, the system time constant τ_0, was estimated to be about 50 msec (24, 26). Recent estimates of the axial resistance in cortical pyramidal neurons suggest values near $R_i = 300$ Ωcm (24, 27). In these studies, C_m was estimated at 0.8 μF/cm^2. Thus, the membrane resistivity in our model was set at 60,000 Ωcm^2 (implying $\tau_0 = 48$ msec). In the axon, R_i was assumed to be 70 Ωcm (e.g., ref. 28). With these specific values, the input resistance at the modeled soma was 122 MΩ, in good agreement with the experimental measurements (29). Second, *active currents* were incorporated in the model. Although cortical pyramidal neurons are endowed with a variety of excitable currents, many of these can be ignored in the present study, which specifically focuses on the most rudimentary mechanism that governs the propagation of a single AP in weakly excitable dendrites. For instance, Markram *et al.* (29) blocked the different voltage-dependent Ca^{2+} currents, showing that these currents affect only negligibly the back propagating AP. Persistent Na^+ current is also not a key player in supporting this AP. Indeed, the measurements made by Stuart and Sakmann (14) from somatic and dendritic membrane patches show that Na^+ current transients inactivate rapidly and return to the baseline following a voltage step. Thus, at the soma and dendrites, the contribution of persistent Na^+ current must be very small. Consequently, in our "minimal model" we utilized only the currents that are essential in simulating the Stuart and Sakmann findings (14), namely the fast-inactivating Na^+ current and the potassium delayed rectifier. It should be emphasized, however, that Ca^{2+} and persistent Na^+ currents probably play an important role in processes such as spike train accommodation, plasticity, etc., which are beyond the scope of this study.

To describe the kinetics of excitable channels, Hodgkin and Huxley formalism (30), at 20°C, was used. To match experimental results of (15, 31, 32), α's and β's for the *dendritic* and *somaic* Na^+ conductance were shifted by +10 mV. m_∞ was described explicitly by $1/\{1 + \exp[(V_{1/2} - V)/K]\}$, with $V_{1/2} = -29.5$ mV and $K = 7.5$ mV. To fit the time course of the Na^+ transient (Fig. 1 *Inset*), τ_h was increased by a factor of 1.6. In the *axon*, τ_h was further increased by a factor of 1.6 and the m_∞ curve was as above with $V_{1/2} = -39.5$ mV. Experimental description of the K^+ conductance is still limited; we based our model on the results of ref. 32 using a single *n*-gate, with $\alpha_n = 0.006 \times (v - 0)/\{1 - \exp[-(v - 20)/9]\}$; $\beta_n = -0.0006 \times (v - 20)/\{1 - \exp[(v - 20)/9]\}$ (see also 33). The ratio $\bar{g}_{Na}/\bar{g}_K$ in soma and axon was kept as in Hodgkin and Huxley model. $E_{Na} = +90$ mV (14) and $E_K = -85$ mV; the resting potential was −70 mV.

Fast excitatory [L-α-amino-3-hydroxy-5-methyl-4-isoxazolepropionate (AMPA)] and inhibitory [γ-aminobutyric acid A and B ($GABA_A$ and $GABA_B$)] inputs were modeled as an α function:

$$g_{AMPA}(t) = g_{peak}(t/t_{peak})\exp(1 - t/t_{peak}). \quad \textbf{[1]}$$

With $g_{peak} = 0.4$ nS, $t_{peak} = 0.3$ msec, and associated reversal potential of 0 mV (34) for the AMPA input. A single AMPA input to a spine, located 200 μm from the soma in the basal tree, produced about 13-mV depolarization at the spine head and about 70 μV at the soma. For the $GABA_A$ input, $g_{peak} = 0.4$ nS at $t_{peak} = 0.2$ msec and for the $GABA_B$ input $g_{peak} = 0.3$ nS at $t_{peak} = 50$ msec. Only the shunting effect of the inhibitory synapses was considered in this study (see Fig. 4) and, therefore, their corresponding reversal potential was not taken into account.

The voltage-dependent, *N*-methyl-D-aspartate (NMDA) conductance input was modeled by:

$$g_{NMDA}(t) = [g_N(\exp(t/\tau_1) - \exp(t/\tau_2)]/ \{1 + \eta[Mg^{2+}]\exp(\gamma V_m)\}, \quad \textbf{[2]}$$

with $g_N = 0.2$ nS; $\tau_1 = 80$ msec; $\tau_2 = 0.67$ msec; $\eta = 0.33$/mM; $[Mg^{+2}] = 2$ mM, and $\gamma = 0.06$/mV (35). The reversal potential for this input was set to 0 mV.

Finally, each dendritic spine receiving excitatory synaptic inputs was modeled as a 0.1 μm × 1 μm cylinder with spherical head diameter of 0.6 μm. Each of these spines received both AMPA and NMDA inputs.

RESULTS

Fig. 2 demonstrates that the experimental results of Stuart and Sakmann (14) cannot be explained solely on the basis of the

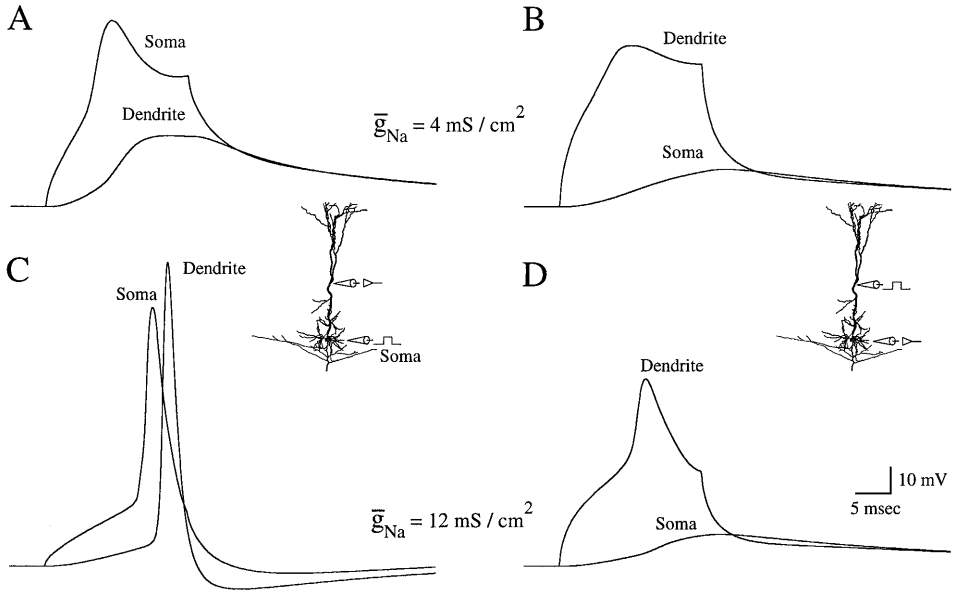

FIG. 2. The morphology of neocortical pyramidal cells *per se* cannot explain why the AP is always initiated first at the axon. (*A*) With a weakly excitable membrane ($\bar{g}_{Na}$ = 4 mS/cm^2) over the whole neuron surface and the measured kinetics of the Na^+ current, a full-blown AP cannot be initiated. In these conditions, a strong (1.3 nA, 40 msec) depolarizing pulse to the modeled soma produced only a small local regenerative response (upper trace). This response propagated decrementally toward the apical dendrite (550 μm from the soma, lower trace and the dendritic electrode in the *Inset*). (*B*) Injection of a 0.6-nA, 40-msec pulse at the dendritic site gave rise to only a small local regenerative response which attenuated significantly toward the soma. (*C*) With uniform $\bar{g}_{Na}$ of 12 mS/cm^2, a soma pulse (300 pA, 40 msec) produced a brief, 90-mV somatic AP; this AP propagated with increased amplitude backwards into the apical dendrite. (*D*) A current pulse (500 pA, 40 msec) to the dendrite initiated a local response first in the dendrite which then attenuated to the soma.

morphological design of neocortical pyramidal neurons. Indeed, with Na^+ channel density of 4 mS/cm^2 over the whole neuron surface (dendrites, soma, and axon), and with the fast inactivating kinetics measured for the sodium current (Fig. 1 *Inset*), a full-blown AP cannot be initiated either from a somatic input (Fig. 2*A*) or from a dendritic input (Fig. 2*B*). With further increase of the channel density (to 12 mS/cm^2), a current input to the soma could generate a 90-mV AP at the soma (Fig. 2*C*). However, in contrast to the experimental results, this AP propagated fully (nondecrementally) into the apical dendrite. When the input was applied to the apical dendrite, a regenerative local response was initiated at the input site (Fig. 2*D*). It then markedly attenuated toward the soma where only a subthreshold depolarization can be seen. We conclude that, to initiate the AP first in the axon, the axon must be more excitable than the soma and dendrites.

Increased excitability (lower threshold) at the axon may result from a higher density of the same Na^+ channels as in the soma and dendrites (36, 37). Alternatively, a smaller channels density in the axon may be sufficient, assuming that the axon is equipped with a different type of Na^+ channels (38). Recent experimental results, suggesting that near the soma the axonal Na^+ channels are not so dense (39) lead us to focus our modeling efforts on the second alternative. Fig. 3 shows that the experimental results of Stuart and Sakmann (14) can be fully reproduced with a relatively low Na^+ channel density in the axon (only 20 times the soma density), assuming that these channels are activated at a more negative potential and have slower kinetics. As seen in Fig. 3*A*, when a depolarizing current pulse was applied to the soma, a rapid, 100-mV AP was observed at the soma. The AP attenuated from the soma to the apical tree, retaining about 50% of its original amplitude at a distance of 550 μm from the soma. When the stimulus was applied to the dendrite, the AP was again initiated first in the soma and then propagated backward into the apical tree (Fig. 3*B*). The shape of the modeled AP at both the soma and the dendrite closely matched the experimental recordings. The agreement included the amplitude and duration of the AP, the voltage threshold at the soma (12 mV), the profile of attenuation of the back-propagating AP (Fig. 3*D*) and its velocity (0.15 m/sec).

As expected, the AP was initiated first in the axon rather than in the soma (Fig. 3*C*). In close agreement with the experimental results of Stuart and Sakmann (personal communication), the axonic AP is larger and briefer than its somatic counterpart. The axonic AP has a prominent after hyperpolarization, and at a distance of 50 μm from the soma, it peaks about 0.5 msec prior to the soma. Fig. 3*C* also shows that the AP propagates *actively* from the soma into the apical dendrite. In the absence of voltage-dependent Na^+ dendritic channels (Fig. 3*C*, dotted line) the back-propagating AP, at a distance of 550 μm from the soma, was 4 times smaller than in the corresponding excitable case (compare with figures 3a and 4a in ref. 14). At this distance, the excitable dendritic Na^+ channels boost the peak of the back-propagating AP by about 40 mV (see also Fig. 3*D*).

In Fig. 4*A* an excitatory input to layer I is simulated. At this distal location, 250 randomly distributed and synchronously activated excitatory synapses (AMPA plus NMDA) on spines were required to initiate an AP at the axon. At a distance of 550 μm from the soma, the peak of the EPSP preceding the back-propagating AP is 18 mV [compare with Stuart and Sakmann (14), figure 2c]. In agreement with the recent study of Stuart and Sakmann (40; see, however, refs. 16 and 41) we found that this layer I EPSP is practically unamplified by the dendritic Na^+ channels. The reason for this is that the activation curve (m_∞^3) of the soma and dendritic Na^+ channels is essentially zero for depolarization smaller than 20 mV. Note, however, that in the experimental conditions, excitatory synaptic inputs to neocortical pyramidal dendrites may be amplified due to voltage-dependent dendritic Ca^{2+} current and somatic persistent Na^+ current (6, 7, 40, 42–44).

What is the effect of the synaptic activity itself on the backward propagating AP? In the *in vivo* conditions, each pyramidal cell is a target for a large number of synapses, each synapse may be activated spontaneously 1–3 times per second

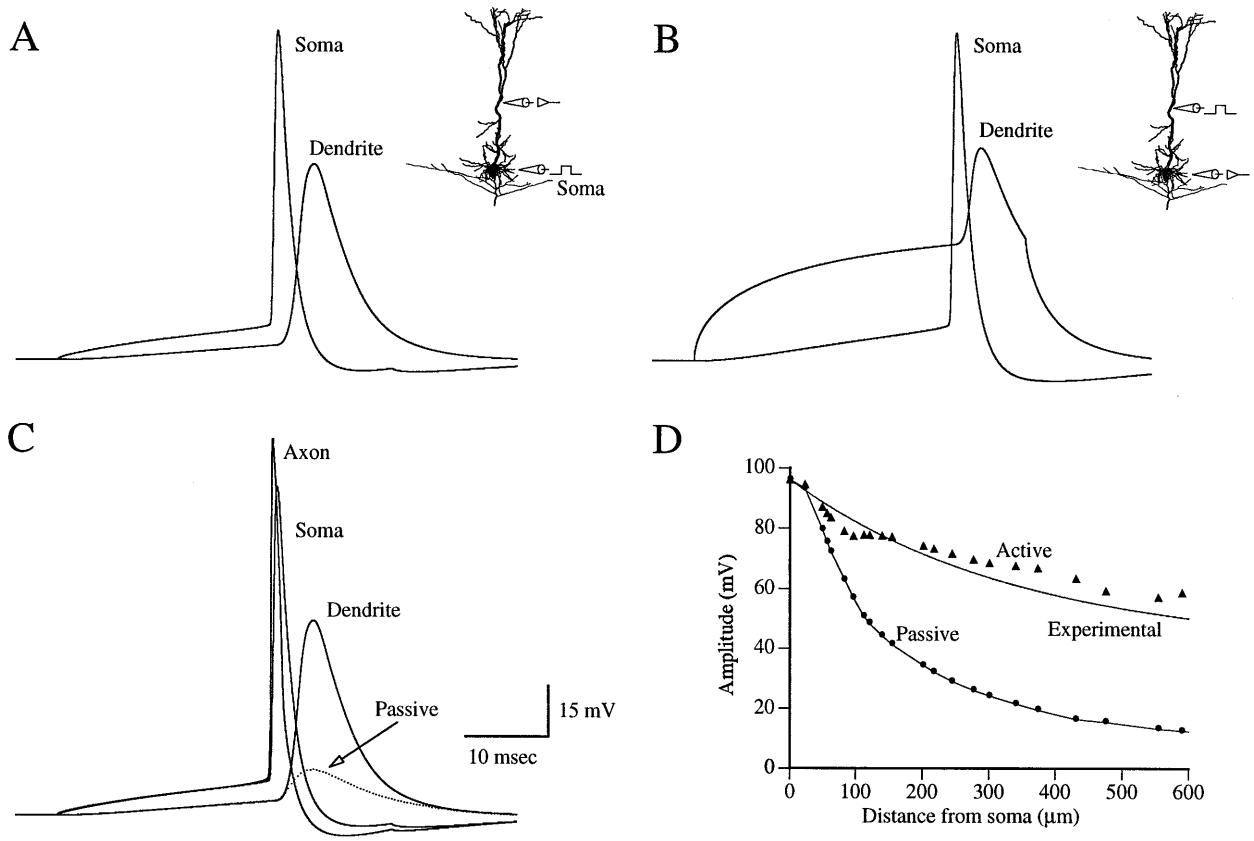

FIG. 3. A model with an excitable axon and weakly excitable dendrites and soma mimics the experimental results. (*A*) A brief, 100-mV, somatic AP is generated in response to a 150-pA, 40-msec pulse to the soma. This AP propagates decrementally into the apical dendrites (recorded at 550 μm from the soma). (*B*) A 300-pA, 40-msec pulse to the apical dendrite initiated the AP at the axon first; this AP then propagated backward into the dendrite. (*C*) The AP is initiated in the axon rather than in the soma (axonal trace recorded 50 μm from the soma). Stimulus parameters are as in *A*. Comparison between the active case (dendritic recording, continuous lines) an the passive case (dendritic recording, dotted line) shows that the AP propagates *actively* back into the dendrite. In the passive case the somatic AP recorded in the active case was used as a voltage command to the soma (a "simulated" AP as in ref. 14). (*D*) Amplitude of the back-propagating AP as a function of distance from the soma. Continuous line, results of Stuart and Sakmann (14); solid triangles, model result; solid circles, passive case. $\bar{g}_{Na}$ in the axon was 140 mS/cm^2. In the dendrites, a linear decrement in $\bar{g}_{Na}$ (from 8 mS/cm^2 at the soma to 4 mS/cm^2 in the dendritic tuft) was used to best fit the experimental results.

(19). This network activity is expected to significantly shunt the postsynaptic cell (20, 21). Indeed, in recent *in vivo* whole cell recordings the effective τ_0 of neocortical pyramidal cells was estimated to be as small as 5 msec, rather than about 50 msec as in the *in vitro* conditions (45). Could such a massive background synaptic activity block the already decremental back-propagating AP? Fig. 4*B* shows that the network activity can finely modulate the back-propagating AP. With background activity of 1.5 Hz (and effective τ_0 reduced from 48 to 17 msec), a 15% decrease of the AP amplitude was observed at a distance of 550 μm from the soma. At 3 Hz it was reduced by 27% (effective τ_0 = 10 msec). We conclude that the amplitude of the back-propagating AP at any given dendritic location can be modulated by the degree of activity in the network of which the neuron is part (see *Discussion*).

Direct recordings from the basal dendrites have not yet been made because of their small dimensions and morphological complexity. In the absence of these data, our model can help by predicting the behavior of the back-propagating AP and of synaptic inputs in these dendrites. If the basal tree is devoid of Na^+ channels, the attenuation of the somatic AP into this tree is quite significant (Fig. 5*A*). Still, about 50% of the basal tree membrane is depolarized by more than 60 mV. Consequently, many of the voltage-dependent Ca^{2+} channels that exist in the basal tree could be activated by a passively attenuated AP (46). If the basal tree is weakly excitable, then the AP could propagate retrogradedly without attenuation (Fig. 5*A*), so activating the voltage-dependent Ca^{2+} channels over the entire basal tree (46). Fig. 5*B* shows the effect of excitatory input to the basal tree. For the synaptic parameters chosen, about 150 simultaneously activated excitatory synapses located randomly on the basal tree (schematic circles), are necessary to initiate an AP in the axon. For this distributed input, the amplitude of the local EPSP at the spine head membrane is about 20 mV, and only slightly smaller in the parent basal dendrite. The somatic AP then propagates fully, reaching the dendritic tips within 1 msec while the long lasting NMDA-mediated receptors are still activated. This may have important consequences for inducing Hebb-like plastic processes in the dendrites (see also ref. 47).

DISCUSSION

The Axon Must Be More Excitable Than the Soma and Dendrites. The experimental finding that dendritic inputs initiate the AP first from the axon suggests that the voltage threshold for AP generation is lower in the axon. Theoretical considerations show that, in principle, the morphology of cortical pyramids, *per se*, can account for this finding. This is the result of the strategic location of the soma and the axon initial segment which implies that an input to the soma will produce a more uniform spatial polarization than an input to a dendritic branch (see figure 2.4 in ref. 1). Theoretically, for a given homogeneously excitable structure, as the spatial distribution of voltage in response to an input is more uniform, the voltage threshold for AP initiation is lower. The lowest

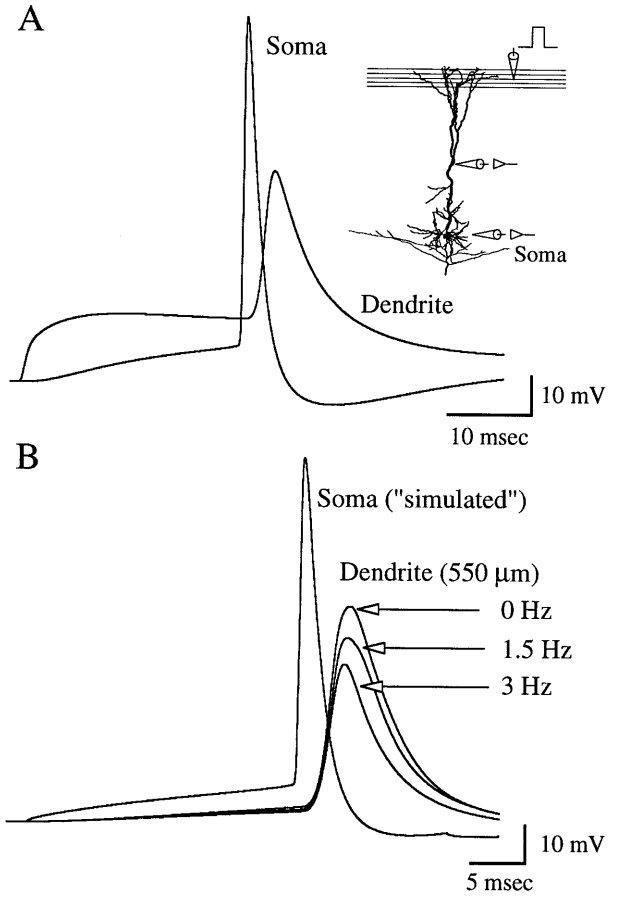

FIG. 4. (*A*) Layer I synaptic input can generate a somatic AP. Layer I synaptic input was modeled by simultaneously activating 250 excitatory (AMPA and NMDA) spiny inputs, randomly distributed on the apical tuft (compare with figure 2c in ref. 14). (*B*) The back-propagating AP can be gradually modulated (rather that blocked) by the background synaptic activity. Spontaneous, asynchronous background synaptic activity was modeled globally as in (20, 21). In this simulation, 8000 excitatory inputs (AMPA plus NMDA), 1000 $GABA_A$, and 1000 $GABA_B$ synaptic inputs were activated. In all cases the same "simulated" AP was imposed on the soma.

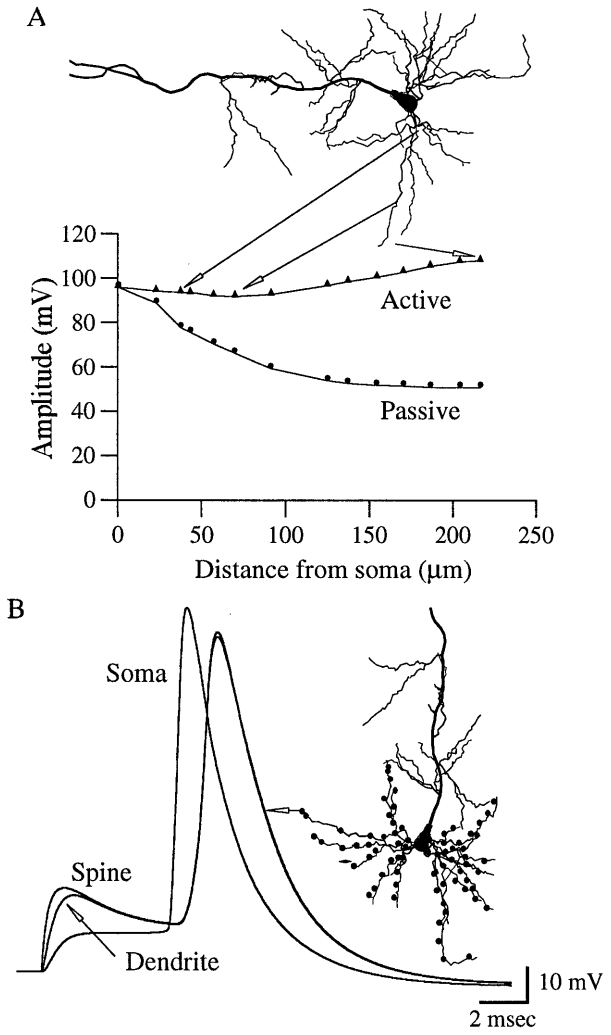

FIG. 5. (*A*) With weakly excitable basal dendrites, the AP is expected to propagate fully back into the dendrites and spines. In the passive case, however, the AP attenuates significantly when spreading from the soma into the relatively short (<250 μm) basal tree. (*B*) Synchronous activation of 150 excitatory synapses was required to initiate an AP in the axon. Synapses located on spines (schematic circles in *Inset*) were distributed randomly over the basal dendrites. The back-propagating AP fully invades the dendritic spines, causing an overshooting potential and, thus, depolarizing the spines membrane beyond the reversal potential of the glutamate-mediated receptors.

threshold is attained under strictly isopotential conditions (uniform polarization). Therefore, the morphology of cortical pyramidal cells favors AP initiation near the soma.

However, for a dendritic input to generate an AP first in the axon and not in the input site, the difference in voltage thresholds between the dendrites and the axon should be larger than the voltage difference due to the attenuation between these two locations. Under this condition a dendritic input can initiate an AP at the axon while remaining subthreshold at the dendrites. With the Na^+ channel density and kinetics reported by Stuart and Sakmann (14) this condition does not hold. Therefore, we had to assume that the Na^+ *current* density in the axon is higher than in the soma and dendrites.

Traditionally, the Na^+ channel density in the axon hillock has been assumed to be very high, but recent studies contradict this notion (39). When we assumed that the same type of Na^+ channels are present in both the dendrites and the axon, then the minimal Na^+ conductance required to initiate the experimental somatic AP was $\approx$1000 mS/cm^2 ($\approx$150 times the soma density, not shown; see also ref. 33). In this study we have shown that a much lower Na^+ channel density in the axon is sufficient, provided that the axon is equipped with a different type of Na^+ channel. In this case the Na^+ channel density in the axon can be reduced to only 20 times that of the soma. We found that it is also possible to reproduce the experimental results assuming that the axon hillock and initial segment of the axon are only weakly excitable (as is the soma) provided that further downstream (>50 μm from the soma) the Na^+ channel density in the axon is 40 times higher than in the soma. Recordings from membrane patches excised from the axon will be required to resolve this issue and further constrain the model.

Model Parameters. Many parameters, both morphological and physiological, determine the behavior of the detailed model presented here. Although the novel method of infrared video-microscopy provides new biophysical data that strongly constrain the model, there are still many unknowns (the membrane properties of spines, the basal tree, and the axon; the value of R_i, etc.). We examined the dependence of the model behavior on a range of these free parameters. For example, the velocity of the back-propagating AP depends critically on the value of R_i. With R_i = 300 Ωcm, the experimentally determined velocity (0.15 m/sec) could be reproduced (see ref. 14), whereas with R_i = 150 Ωcm the velocity increased to 0.21 m/sec. Also, the experimental results demonstrate clearly that the back-propagating AP decrements very

gradually along the apical tree. Exploration of the model shows that, with uniform Na^+ channel density in the apical tree, the AP either drops too steeply with distance and then remains almost constant, or (assuming somewhat higher uniform density) the AP does not decrement at all (see also figure 10A in ref. 48). A model with a moderate decrement in Na^+ channel density (from 8 mS/cm^2 at the soma to 4 mS/cm^2 at distal regions) best fitted the experimental results (Fig. 3*D*). Clearly, our current model is not unique, yet it allows us to reject certain possibilities and highlight important principles that govern signal processing in weakly excitable dendrites.

Modulation of Back-Propagating AP by Network Activity. As the density of excitable channels decreases, the AP becomes more susceptible to morphological inhomogeneities and to synaptic shunt. Because the back-propagating AP is supported by a low density of Na^+ channels, network activity can control its amplitude in a graded manner, and thus determine the extent to which the AP invades the dendritic tree, as well as which subtrees will be invaded (49). With the experimentally based parameters used in this study, the decremental back-propagating AP is rather resistant to synaptic shunt and only a relatively powerful input can dampen it in a significant way.

Forward Synaptic Integration Versus Backward Active Propagation. The higher threshold in the dendrites ensures that they will not fire a local sodium AP during dendritic input. Furthermore, only a small fraction of the dendritic channels are likely to be activated during excitatory synaptic input (40). In contrast, large depolarization, such as the somatic AP, does activate dendritic Na^+ channels and, consequently, the back-propagating AP is boosted. Indeed, neurons with weak dendritic excitability, and more excitable axon, function as unique electrical devices. In the forward direction, synaptic inputs are integrated without the interference of local dendritic APs. In the backward direction, the weak dendritic excitability helps to transmit a global message from the axon to the whole dendritic tree.

Many thanks to Henry Markram and Greg Stuart for their valuable input, to Michael Hines for his indispensable help with his NEURON simulator, and to Anirudh Gupta for helping in reconstructing the modeled neurons. This work was supported by the U.S. Office of Naval Research and by the U.S.–Israeli Binational Science Foundation.

1. Rall, W. (1989) in *Methods in Neuronal Modeling; From Synapses to Networks*, eds. Koch, C. & Segev, I. (MIT Press, Cambridge, MA), pp. 9–62.
2. Segev, I., Rinzel, I. & Shepherd, G. M. (1995) *The Theoretical Foundation of Dendritic Function* (MIT Press, Cambridge, MA).
3. Llinás, R. & Sugimori, M. (1981) *J. Physiol. (London)* **305,** 197–213.
4. Ross, W. N. & Werman, R. (1987) *J. Physiol. (London)* **389,** 319–336.
5. Jaffe, D. B., David B., Johnston, D., Lasser-Ross, N., Lisman, J. E., Miyakawa, H. & Ross, W. N. (1992) *Nature (London)* **357,** 244–246.
6. Yuste, R., Gutnick, M., Saar, D., Delaney, K. & Tank, D. (1994) *Neuron* **13,** 23–43.
7. Turner, R. W., Maler, L., Deerinck, T., Levinston, S. R. & Ellisman, M. H. (1994) *J. Neurosci.* **14,** 6452–6471.
8. Yuste, R. & Denk, W. (1995) *Nature (London)* **375,** 682–684.
9. Rall, W. & Segev, I. (1987) in *Synaptic Function*, eds. Edelman, G. M., Gall, W. F. & Cowan, W. M. (Wiley, New York), pp. 605–636.
10. Mel, B. W. (1993) *J. Neurophysiol.* **70,** 1086–1101.
11. Softky, W. (1994) *Neuroscience* **58,** 13–41.
12. Bernander, O., Koch, C. & Douglas, R. J. (1994) *J. Neurophysiol.* **72,** 2743–2753.
13. Stuart, G. J., Dodt, H.-U. & Sakmann, B. (1993) *Pflügers Arch. Gesamte Physiol.* **423,** 511–518.
14. Stuart, G. J. & Sakmann, B. (1994) *Nature (London)* **267,** 69–72.
15. Magee, J. C. & Johnston, D. (1995) *J. Physiol. (London)* **487,** 67–90.
16. Magee, J. C. & Johnston, D. (1995) *Science* **268,** 301–304.
17. Spruston, N., Schiller, Y., Stuart, G. & Sakmann, B. (1995) *Science* **268,** 297–300.
18. Hausser, M., Stuart, G., Rocca, C. & Sakmann, B. (1995) *Neuron* **15,** 637–647.
19. Abeles, M. (1991) *Corticonics, Neural Circuits of the Cerebral Cortex* (Cambridge Univ. Press, Cambridge).
20. Bernander, Ö., Douglas, R. J., Martin, K. A. C. & Koch, C. (1991) *Proc. Natl. Acad. Sci. USA* **88,** 11569–11573.
21. Rapp, M., Yarom, Y. & Segev, I. (1992) *Neural Comp.* **4,** 518–533.
22. Hines, M. (1989) *Int. J. Biomed. Comput.* **24,** 55–68.
23. Larkman, A. (1991) *J. Comp. Neurol.* **306,** 332–343.
24. Stratford, K., Mason, A., Larkman, A., Major, G. & Jack, J. J. B. (1989) in *The Computing Neuron,* eds. Durbin, R., Miall, C. & Mitchison, G. (Addison-Wesley, London), pp. 296–321.
25. Angelides K. J. & Benke, T. A. (1995) *4th IBRO Congr. Neurosci. Abstr.*, S17.9.
26. Stuart, G. & Spruston, N. (1995) *Curr. Opin. Neurobiol.* **5,** 389–394.
27. Major, J., Larkman, A. U., Jones, P., Sakmann, B. & Jack, J. J. (1994) *J. Neurosci.* **14,** 4613–4638.
28. Traub, R. D. (1995) *J. Comput. Neurosci.* **2,** 291–298.
29. Markram, H., Helm, P. J. & Sakmann, B. (1995) *J. Physiol. (London)* **485,** 1–20.
30. Hodgkin, A. L. & Huxley, A. F. (1952) *J. Physiol. (London)* **108,** 37–77.
31. Cummins, T., Xia, Y. & Haddad, G. G. (1994) *J. Neurophysiol.* **71,** 1052–1064.
32. Hamill, O. P., Huguenard, J. R. & Prince, D. A. (1991) *Cereb. Cortex* **1,** 48–61.
33. Mainen, Z. F., Joerges, J., Huguenard, J. R. & Sejnowski, T. J. (1995) *Neuron* **15,** 1427–1439.
34. Stern, P., Edwards, F. A. & Sakmann, B. (1992) *J. Physiol. (London)* **449,** 247–278.
35. Jahr, C. E. & Stevens, C. F (1990) *J. Neurosci.* **10,** 1830–1837.
36. Moore, J. W., Stockbridge, N. & Westerfield, M. (1983) *J. Physiol. (London)* **336,** 301–311.
37. Wollner, D. A. & Catterall, W., A. (1986) *Proc. Natl. Acad. Sci. USA* **83,** 8424–8428.
38. Westenbroek, R. E., Merrick, D. M. & Catterall, A. (1989) *Neuron* **3,** 695–704.
39. Colbert, C. M. & Johnston, D. (1995) *Soc. Neurosci. Abstr.* **21,** 684.2.
40. Stuart, G. & Sakmann, B. (1995) *Neuron* **15,** 1065–1076.
41. Cauller, L. J. & Connors, B. W. (1992) in *Single Neuron Computation*, eds. McKenna, T., Davis, J. & Zornetzer, S. F. (Academic, Boston), pp. 199–230.
42. Gutfreund Y., Yarom., Y. & Segev, I. (1995) *J. Physiol. (London)* **483,** 621–640.
43. Markram, H. & Sakmann, B. (1994) *Proc. Natl. Acad. Sci. USA* **91,** 5207–5211.
44. Fleidervish, I., Friedman, A. & Gutnick, M. (1996) *J. Physiol. (London)*, in press.
45. Chen, D. -F. & Fetz, E. E. (1993) *Soc. Neurosci. Abstr.* **19,** 781.
46. Schiller, J., Helmchen, F. & Sakmann, B. (1995) *J. Physiol. (London)* **487,** 583–600.
47. Rhodes, P. (1996) *J. Neurosci.*, in press.
48. Kim, H. G. & Connors, B. W. (1995) *J. Neurosci.* **13,** 5301–5311.
49. Kim, H. G., Breierlein, M. & Connors, B. W. (1995) *J. Neurophysiol.* **4,** 1810–1814.